Hindawi Publishing Corporation
Advances in OptoElectronics
Volume 2011, Article ID 963068, 10 pages
doi:10.1155/2011/963068

Research Article

Substitution of Carbazole Modified Fluorenes as π-Extension in Ru(II) Complex-Influence on Performance of Dye-Sensitized Solar Cells

Malapaka Chandrasekharam,[1] Ganugula Rajkumar,[2] Thogoti Suresh,[1] Chikkam Srinivasa Rao,[1] Paidi Yella Reddy,[2] Jun-Ho Yum,[3] Mohammad Khaja Nazeeruddin,[3] and Michael Graetzel[3]

[1] *Inorganic and Physical Chemistry Division, Indian Institute of Chemical Technology, Uppal Road, Tarnaka, Hyderabad 500 607, India*
[2] *Aisin Cosmos R&D Co. Ltd., Indian Institute of Chemical Technology, Uppal Road, Tarnaka, Hyderabad 500 607, India*
[3] *Laboratory of Photonics and Interfaces, Swiss Federal Institute of Technology (EPFL), 1015 Lausanne, Switzerland*

Correspondence should be addressed to Malapaka Chandrasekharam, csmalapaka@yahoo.com

Received 30 April 2011; Accepted 31 May 2011

Academic Editor: Surya Prakash Singh

A new high molar extinction coefficient ruthenium(II) bipyridyl complex "*cis*-Ru(4,4′-bis(9,9-dibutyl-7-(3,6-di-tert-butyl-9H-carbazol-9-yl)-9H-fluoren-2-yl)-2,2′-bipyridine)(2,2′-bipyridine-4,4′-dicarboxylic acid)$(NCS)_2$, **BPFC**" has been synthesized and characterized by FT-IR, ^{1}H-NMR, and ESI-MASS spectroscopes. The sensitizer showed molar extinction coefficient of $18.5 \times 10^3\,M^{-1}cm^{-1}$, larger as compared to the reference **N**719, which showed $14.4 \times 10^3\,M^{-1}cm^{-1}$. The test cells fabricated using **BPFC** sensitizer employing high performance volatile electrolyte, (**E**01) containing 0.05 M I_2, 0.1 M LiI, 0.6 M 1,2-dimethyl-3-*n*-propylimidazolium iodide, 0.5 M 4-*tert*-butylpyridine in acetonitrile solvent, exhibited solar-to-electric energy conversion efficiency (η) of 4.65% (short-circuit current density (J_{SC}) = 11.52 mA/cm^2, open-circuit voltage (V_{OC}) = 566 mV, fill factor = 0.72) under Air Mass 1.5 sunlight, lower as compared to the reference **N**719 sensitized solar cell, fabricated under similar conditions, which exhibited η-value of 6.5% (J_{SC} = 14.3 mA/cm^2, V_{OC} = 640 mV, fill factor = 0.71). UV-Vis measurements conducted on TiO_2 films showed decreased film absorption ratios for **BPFC** as compared to those of reference **N**719. Staining TiO_2 electrodes immediately after sonication of dye solutions enhanced film absorption ratios of **BPFC** relative to those of **N**719. Time-dependent density functional theory (TD-DFT) calculations show higher oscillation strengths for 4,4′-bis(9,9-dibutyl-7-(3,6-di-tert-butyl-9H-carbazol-9-yl)-9H-fluoren-2-yl)-2,2′-bipyridine relative to 2,2′-bipyridine-4,4′-dicarboxylic acid and increased spectral response for the corresponding **BPFC** complex.

1. Introduction

Dye sensitized solar cells (DSSCs) attracted intense attention among scientific as well as industrial organizations because of their high photon-to-electricity conversion efficiency and low cost compared to traditional photoelectrochemical cells [1–5]. Since Graetzel introduced the first highly efficient nanocrystalline TiO_2 sensitized solar cell based on ruthenium(II) bipyridyl complex, **N**3 as sensitizer, there have been several modifications to improve the overall performance of the test cell devices [6–22]. Among all the components employed in DSSC, sensitizer plays a key role in photovoltaic performance in respect of efficiency and long-term durability. The important tunable properties of sensitizers for high efficient DSSCs are broad absorption (400 to 900 nm) and high molar extinction coefficient (thin films and solid state DSSCs), thermal and photochemical stability (long durable), compatibility with TiO_2 semiconductor conduction band (efficient electron injection) and redox electrolyte (efficient dye regeneration), nonplanar molecular structure, and so forth [6, 8, 22–24]. Thiophene containing oligomers have been extensively explored as the active organic materials

for OFET applications due to the ease in chemical modification of the structures, allowing fine-tuning their optical and electronic properties [25]. They exhibit high field-effect mobility, which have been related to both, the close packing through π-interactions and the high degree of local order of molecules [26]. Thiphene oligomers display poor stability especially in the solid state, limiting their practical applications, where as fluorine-based oligomers showed both improved stability and lower HOMO level as compared to thiophene oligomers. Endcaping of oligofluorenes with diphenylamino group has been shown to offer advantages in terms of lowering their first ionization potentials, enhancing thermal stability and inducing good amorphous morphological stability [27]. Thus, fluorene unit as the core is known to display interesting chemical and electronic characteristics. We have been engaged in our laboratory to synthesize durable and high efficient new organic, phthalocyanine as well as ruthenium(II) bipyridyl dyes, [22–24, 28–32] and came across a report of super sensitizer, where carbazole was incorporated on ancillary bipyridyl through conjugation of thiophene moiety [33]. And as a part of our continued efforts in this area of research, we became interested to synthesize a new ruthenium(II) bipyridyl complex **BPFC** by introducing 4,4′-bis(9,9-dibutyl-7-(3,6-di-*tert*-butyl-9H-carbazol-9-yl)-9H-fluoren-2-yl)-2,2′-bipyridine as an ancillary ligand, and the influence of increased conjugation length on photovoltaic performance and thermal stability was evaluated relative to **N**719 sensitizer. Multiple performance increasing features such as alkyl groups (n-butyl and t-butyl), triarylamine equivalent (carbazole), biphenyl group in fluorene as extended conjugation have been incorporated in the new ruthenium(II) complex **BPFC** for achieving better overall performance.

2. Results and Discussion

2.1. Synthesis. Structure of the new ruthenium(II) bipyridyl sensitizer is shown in Figure 1 and the series of steps involved in synthesis of the complex are illustrated in Scheme 1. The new substituted π-conjugated ancillary bipyridyl ligand "4,4′-bis(9,9-dibutyl-7-(3,6-di-tert-butyl-9H-carbazol-9-yl)-9H-fluoren-2-yl)-2,2′-bipyridine" (**L**1) was prepared in accordance to the reported classical reactions. Fluorene, procured from Sigma-Aldrich, was directly used in the bromination reaction to obtain 2-bromofluorene (1), which was subjected to bromine lithium exchange reaction with *n*-butyllithium (*n*-BuLi) followed by addition of *n*-butylbromide to obtain 2-bromo-9,9-dibutyl-9H fluorene (2). This was further reacted with triisopropylborate in presence of *n*-BuLi to form 9, 9-dibutyl-9H-fluoren-2-ylboronic acid (3). The boronic acid derivative was coupled with 4,4′-dibromo-2,2′-bipyridine under palladium catalyzed Suzuki conditions to afford 4,4-bis(9,9-dibutyl-9H-fluorene-2-yl)-[2, 2] bipyridine. The bipyridyl derivative thus obtained was treated with elemental iodine to afford 4,4′-bis(9,9-dibutyl-7-iodo-9H-fluoren-2-yl)-2,2′-bipyridine (5). The diiodo compound, on further reaction with 3,6-di-*tert*-butyl-9H-carbazole resulted crude **L**1, which was purified on silica gel column chromatography to obtain pure **L**1. The ancillary ligand **L**1 was subjected to complexation with $[RuCl_2p\text{-cymene}_2]_2$ in DMF and followed by addition of 2,2′-bipyridine-4,4′-dicarboxylic acid and excess ammonium thiocyanate resulted the formation of crude **BPFC**. The complex was purified on Sephadex LH-20 column chromatography. The intermediates formed during the several classical reactions and the final ruthenium complex are characterized by FT-IR, ^{1}H-NMR, UV-Vis and ESI-MASS spectroscopes. The reference sensitizer, **N**719, was synthesized in accordance to the procedure reported.

2.1.1. Synthesis of 2-Bromofluorene (1). To a solution of fluorene (0.500 g, 1.8 mmoL) in dry acetone was added N-bromosuccinimide (0.320 g, 1.8 mmol) under nitrogen atmosphere. After maintaining at 80°C for 3 hours, cool to room temperature and ice water was added and then extracted with dichloromethane. The crude compound was purified on silica gel column chromatography using hexane/ethyl acetate mixture in 9/1 as eluent. Yield: 90% ^{1}H NMR (δH/ppm in $CDCl_3$): 7.75–7.65 (m, 3H), 7.45–7.20 (m, 4H). Chemical formula $C_{13}H_{10}Br$: ESI-MS: Calcd for $(M + H)^+$: 246, found: 246 (28%).

2.1.2. Synthesis of 2-Bromo-9,9-Dibutyl-9H-Fluorine (2). To a mechanically stirred mixture of 2-bromofluorene (0.980 g, 4 mmol), powdered KOH (1.200 g, 20 mmol), KI (0.066 g, 0.4 mmol), and DMSO (20 mL) were added and cooled to 10°C. Bromobutane (1.076 mL, 10 mmol) was added drop wise over 45 minutes. The color of the reaction mixture turned from red to light purple. After the temperature increased to 20°C, the reaction mixture was left over night, with stirring, poured into water and the precipitate obtained was extracted into dichloromethane. The organic extract was washed with brine solution and water and then concentrated with rotavapour. The compound was purified on silica gel column chromatography using hexane/ethyl acetate mixture in 9/1 as eluent. Yield: 90% ^{1}H NMR (δH/ppm in $CDCl_3$): 7.75–7.65 (m, 3H), 7.45–7.20 (m, 4H), 1.99 (m, 2H), 1.50 (t, 4H), 1.30 (t, 4H), 0.73 (t, 6H), 0.60 (s, 6H). Chemical formula $C_{21}H_{25}Br$: ESI-MS: Calcd for $(M + H)^+$: 357, found: 357 (100%).

2.1.3. Synthesis of 9,9-Dibutyl-9H-Fluoren-2-Ylboronic Acid (3). To a 100 mL two neck glass flask containing **2** (0.500 g, 1.4 mmol) in dry THF (20 mL) and a magnetic stirrer bar at –78°C, *n*-BuLi (1.05 mL, 1.05 mmol) was added under nitrogen atmosphere while maintaining good stirring. After stirring for 1 hour, triisopropylborate (0.484 mL, 2.1 mmol) was added. After stirring for further 2 hours, the reaction mixture was first quenched with water and then aqueous HCl (6 M, 20 mL) was added drop wise fashion until the solution turned acidic and then extracted with dichloromethane. The combined organic layers were dried over anhydrous sodium sulphate and concentrated with rotavapour. Purification was carried out by column chromatography on silica gel using hexane/ethyl acetate mixture (4/6 v/v) as eluent. Yield: 50%. ^{1}H NMR (δH/ppm in $CDCl_3$): 7.70 (d, 1H), 7.62 (s, 1H), 7.42–7.27 (m, 5H), 1.99 (s, 2H), 1.92 (m, 4H), 1.10 (t, 4H),

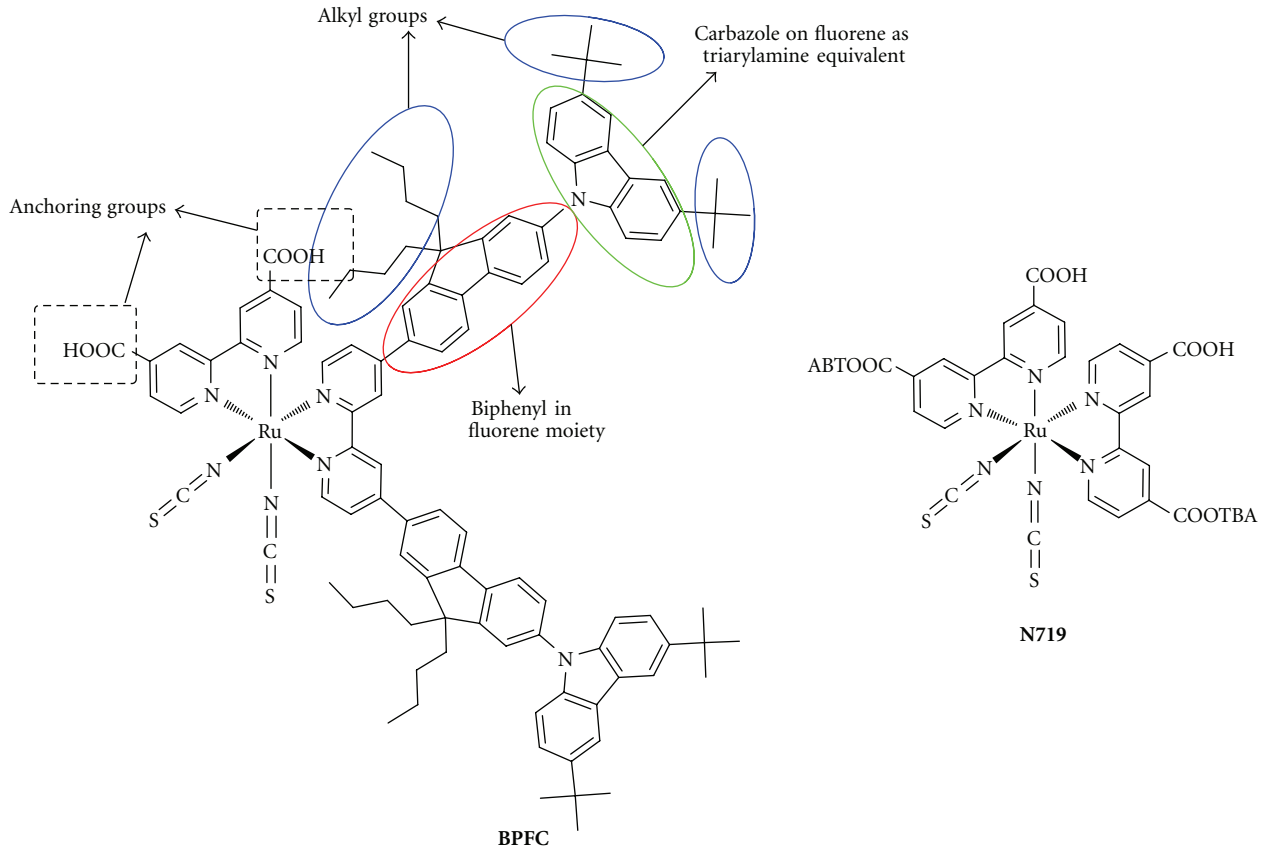

Figure 1: Structure of the new ruthenium(II) sensitizer.

0.73 (t, 6H), 0.60 (s, 6H). Chemical formula $C_{21}H_{27}BO_2$, ESI-MS: Calcd for $(M + H)^+$: 323, found: 323 (100%).

2.1.4. Synthesis of 4,4-Bis(9,9-Dibutyl-9H-Fluorene-2-yl)-[2, 2]-Bipyridine (4). In a 25 mL one-necked round bottom flask equipped with a condenser were placed **3** (0.440 g, 1.375 mmol), barium hydroxide octahydrate (1.355 g, 4.297 mmol), and palladium tetrakis triphenyl phosphine (0.106 g, 0.091 mmol). The reaction flask was evacuated and filled with nitrogen gas, and is charged with 1.4-dioxane (4 mL), water (1.35 mL) and 4,4′-dibromo-2,2′-bipyridine (0.180 g, 0.573 mmol). The reaction mixture was refluxed for 24 hours under nitrogen gas and then cooled to room temperature. The dioxane was removed and the contents were poured into dichloromethane, the precipitate was removed through filter paper, and the organic layer was washed with 1 M-NaOH aqueous solution, NaCl (100 mL) and dried over sodium sulphate. After concentration on rotavapour, small quantity of methanol was added. The precipitate formed was filtered and purified on column chromatography with silica gel using mixture dichlorometh -ane/methanol, (9/1 v/v) to obtain the pure product as pale yellow solid Yield 50%. ^{1}H NMR (500 MHz, $CDCl_3$) 8.70 (d, 1H), 8.63 (s, 1H), 7.80 (d, 1H), 7.60 (d, 1H), 7.29–6.63 (m, 6H), 2.0 (m, 4H), 1.50 (m, 4H), 1.10 (m, 4H), 0.86 (s, 6H). Chemical formula ($C_{52}H_{56}N_2$), ESI-MS: Calcd for $(M + H)^+$: 709, found: 709 (70%).

2.1.5. Synthesis of 4,4-Bis(9,9-Dibutyl-7-Iodo-9H-Fluorene-2-yl)-[2, 2]-Bipyridine (5). A mixture of **4** (0.200 g, 0.282 mmol), iodine (0.172 g, 0.677 mmol), conc H_2SO_4 (0.036 mL) and water (0.013 mL) in glacial acetic acid (10 mL) were taken into 1-neck 100 mL round bottom flask. Then, the mixture was stirred at 80°C under nitrogen gas for 4 hours, and then, the reaction mixture was cooled to room temperature. The solution was poured into large amount of ice cool water. The resulting mixture was extracted with dichloromethane and then washed with water and then dried over Na_2SO_4 and concentrated on rotavapour, small quantity of methanol was added. The precipitate formed was separated and purified on column chromatography with silica gel using mixture (DCM/methanol, 9/1) to obtain the pure product as pale yellow solid Yield 45%. ^{1}H NMR (δH/ppm in $CDCl_3$) 8.8 (d, 2H), 8.75 (s, 2H), 7.6–7.8 (m, 8H), 7.5 (d, 2H), 7.25 (s, 4H), 2.0 (t, 8H), 1.15 (m, 16H), 0.78 (t, 12H). Chemical formula ($C_{52}H_{54}I_2N_2$), ESI-MS: Calcd for $(M + H)^+$: 961, found: 961 (75%).

2.1.6. Synthesis of 4,4-Bis(9,9-Dibutyl-7,7 Di tert-butyl Carbazole-9H-Fluorene-2-yl)-[2, 2]-Bipyridinyl (6). In a 2-neck 250 mL round bottom flask containing 4,4-bis(9,9-dibutyl-7-iodo-9H-fluorene-2-yl)-[2,2]-bipyridinyl (0.100 g, 0.104 mmol), di-*tert*-butyl carbazole (0.087 g, 0.312 mmol), copper bronze (0.005 g, 0.084 mmol), and K_2CO_3 (0.067 g, 0.487 mmol) freshly distilled nitrobenzene was added, and

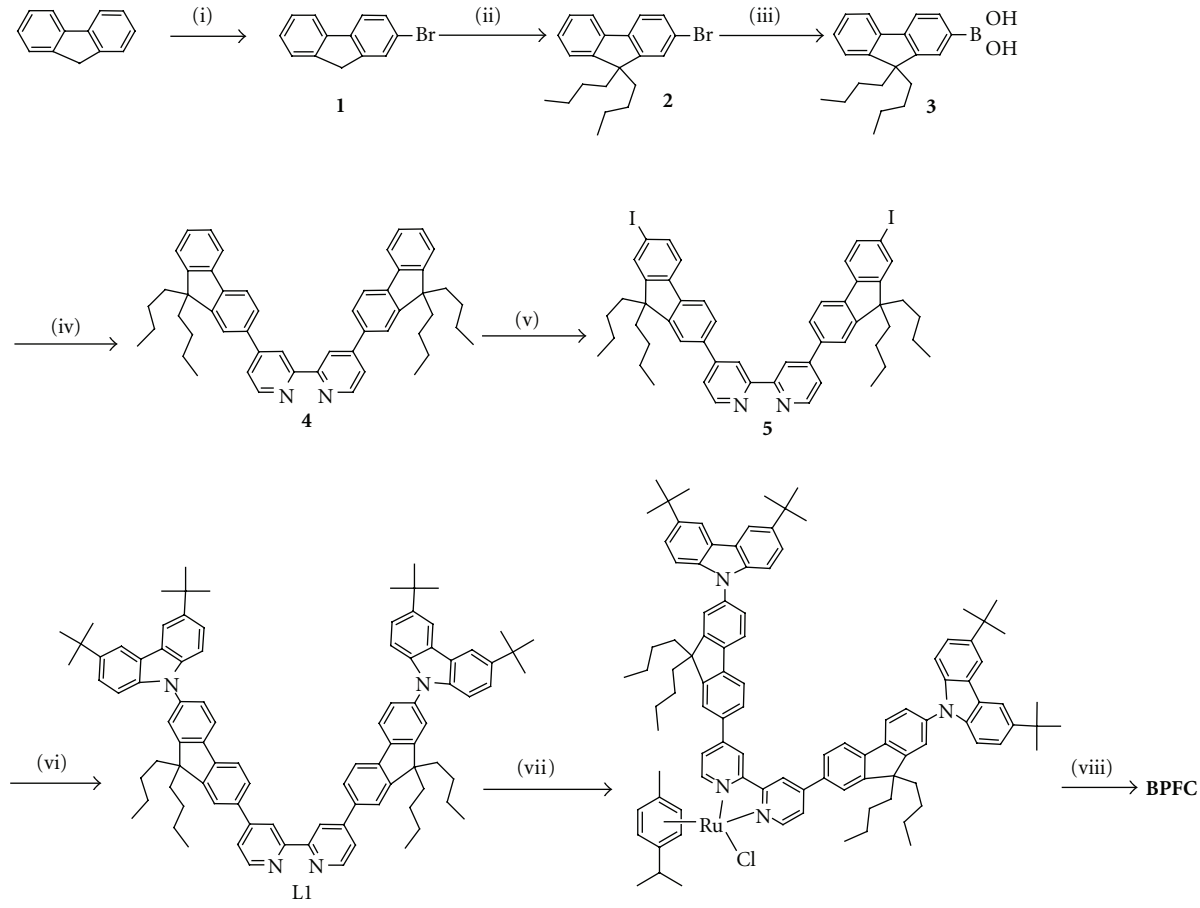

Scheme 1: Synthesis route for **BPFC**; (i) N-bromosuccinimide, acetone at 60°C 3 hours; (ii) bromobutane, powdered KOH, KI and DMSO, RT 12 hours; (iii) *n*-BuLi, Triisopropyl borate, THF, 2M HCl, −78°C, 4 hours; (iv) 4,4′-dibromo-2,2′-bipyridine, $Ba(OH)_2 \cdot 8H_2O$, $Pd(PPh_3)_4$, dioxane/water, reflux, 24 hours; (v) Iodine, conc. H_2SO_4, HIO_4, H_2O, AcOH, 80°C, 4 hours; (vi) 3,6-di-*tert*-butyl-9H-carbazole, Cu Bronze, K_2CO_3, Nitrobenzene, reflux, 24 hours; (vii) $[Ru(p\text{-cymene})_2Cl_2]_2$, DMF, 60–70°C; (viii) 4,4′-dicarboxy-2,2′-bipyridine, NH_4NCS, DMF, 8 hours, reflux.

the contents were stirred under N_2 atmosphere under reflux at 210°C for 24 hours. After cooling to room temperature the reaction mixture was concentrated on the rotavapour for complete removal of nitrobenzene. The crude reaction mixture was then subjected to purification on silica gel column chromatography using ethyl acetate/methanol (9/1) as eluent, 45% yield. ^{1}H NMR (δH/ppm in $CDCl_3$) 8.81 (d, 2H), 8.79 (s, 2H), 7.54–7.85 (m, 18H), 7.35 (d, 4H), 7.12 (d, 4H), 2.0 (t, 8H), 1.50 (m, 16H), 1.35 (s, 36H), 0.86 (t, 12H). Chemical formula ($C_{92}H_{102}N_4$), ESI-MS: Calcd for $(M)^+$: 1263, found: 1263 (100%).

2.1.7. Synthesis of Ruthenium(II) Complex. Compound **6** (0.100 g, 0.079 mmol) and dichloro (*p*-cymene) ruthenium(II) dimer (0.024 g, 0.039 mmol) in DMF were heated at 60°C for a period of 4 hours under nitrogen in dark. Subsequently 4,4′-dicarboxylic acid-2,2′-bipyridine (0.019 g, 0.079 mmol) was added and the reaction mixture was heated to 140°C for another 4 hours. To the resulting dark green solution, solid NH_4NCS (0.180 g, 2.37 mmol) was added and then the reaction mixture was further heated for another 4 hours at 140°C. After rotaevaporation of DMF, water (250 mL) was added to get precipitate. The precipitate was kept in refrigerator overnight, filtered and washed with distilled water and then dried in vacuum desiccator. The crude compound was dissolved in methanol and dichloromethane mixture and further purified on sephadex LH-20 column using methanol/dichloromethane mixture (3/2 v/v) as eluent. The main band was collected and concentrated with rotavapour. Yield: 65%. ^{1}H NMR (δH/ppm in CD_3OD + $CDCl_3$) 9.48 (d, 1H), 9.39 (d, 1H), 8.82 (s, 1H), 8.69 (s, 1H), 8.56 (s, 1H), 8.41 (s, 1H), 7.30–8.30 (m, 29H), 7.18 (d, ^{1}H), 1.8 (t, 8H), 1.35 (s, 36H), 1.15 (m, 16H), and 0.85 (t, 12H). Chemical formula $RuC_{109}H_{116}N_8O_4S_2$, ESI-MASS: Calcd for $(M + H)^+$: 1768, found: 1768 (72%).

2.2. Fabrication of Test Cells. Fluorine-doped SnO_2 (FTO) conducting glass plates (Nippon Sheet Glass, 4 mm thick, 8 Ω/sq) were cleaned with a detergent solution followed by rinsing with water and ethanol and then treated in a UV-O_3 system to remove organics and other contaminants. A compact layer, which will facilitate a good mechanical contact

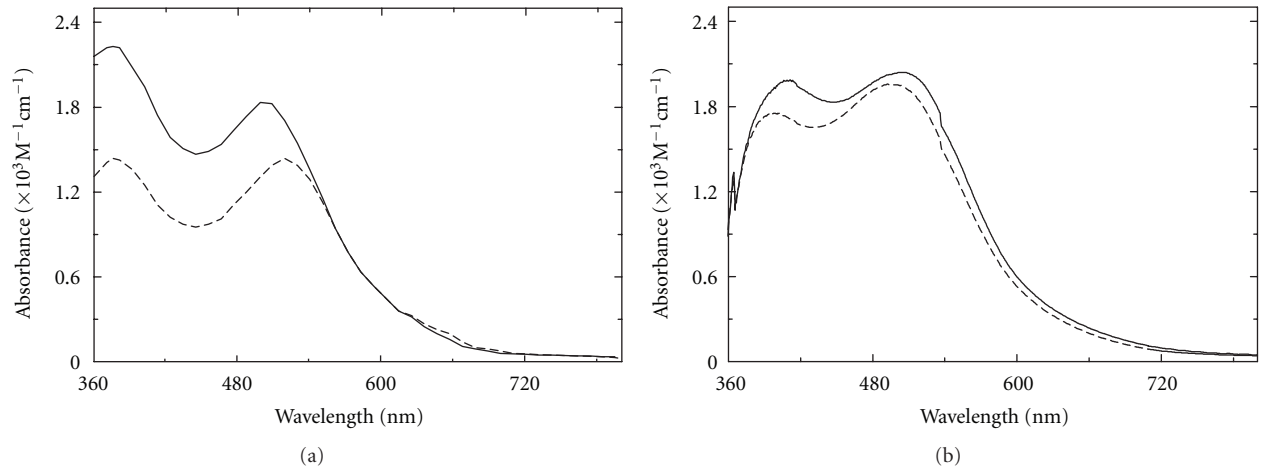

Figure 2: Absorption spectrum of **BPFC** (—) relative to **N**719 (----) (a) equi-molar in ethanol (b) on TiO_2 films.

between the nanocrystalline TiO_2 and the conducting FTO matrix, was coated over the cleaned plates using a 40 mM $TiCl_4$ aqueous solution, and then, the plates were heated at 70°C for 30 minutes. The working electrodes are composed with 9 μm thickness of 18 nm TiO_2 particles (D18T) as transparent layer over which 4.8 μm thickness of 400 nm anatase TiO_2 particles (CCIC, HPW-400) as scattering layer. The TiO_2-coated films were gradually heated under an air flow at 325°C for 5 minutes, at 375°C for 5 minutes, at 450°C for 15 minutes, and at 500°C for 15 minutes. While cooling, when the temperature attained to around 90°C, the electrodes were immersed in 0.3 mM dye solutions of ethanol and soaked for 16 hours under the dark. The dye-sensitized TiO_2 electrodes were rinsed with ethanol to remove the unadsorbed dye molecules and then dried under nitrogen gas. The counter electrodes were prepared by coating an FTO plate (TEC 15, 2.2 mm thickness, Libbey-Owens-Ford Industries) with a drop of H_2PtCl_6 solution (2 mg of Pt in 1 mL of ethanol) and heating it at 430°C for 15 minutes. The dye sensitized TiO_2 electrode and Pt counter electrode were assembled into a sealed sandwich type cell by heating with a hot-melt surlyn film (Surlyn 1702, 25 μm thickness, Du-Pont) as a spacer in-between the electrodes. The liquid electrolyte of **E**01 (I_2 0.05 M, LiI 0.1 M, DMPII 0.6 M, and TBP 0.5 M in acetonitrile) was filled through the predrilled hole present on the counter electrode, and then, the hole was sealed with a Surlyn disk and a thin glass to avoid leakage of the electrolyte.

2.3. Absorption and Emission Properties. The electronic absorption spectrum of **BPFC** sensitizer recorded in ethanol is shown in Figure 2(a), and the spectrum was compared with that of the reference **N**719 sensitizer. The complex exhibited one absorption band at longer wavelength region and a shoulder type band in short wavelength region. The molar extinction coefficient of low-energy absorption band of **BPFC** is 18.5×10^3 M^{-1} cm^{-1}, which is larger as compared to that of reference **N**719 sensitizer that showed molar extinction coefficient of 14.4×10^3 M^{-1} cm^{-1}. Compared to **N**719, the increase in π-conjugation length by introduction of 4, 4′-bis(9,9-dibutyl-7-(3,6-di-tert-butyl-9H-carbazol-9-yl)-9H-fluoren-2-yl)-2,2′-bipyridine in **BPFC** complex increases the molar extinction coefficient and the spectral response of the new complex. The high-energy shoulder type absorption band of the complex with increased molar extinction coefficient could be attributed to the π-π^* transitions of fluorene segments which exhibit strong absorption at around 400 nm.

The high-energy absorption band of ruthenium(II)-bipyridyl complexes is contributed by two components: one is metal to ligand charge transfer transition, while the other one is π-π^* transitions of the ancillary bipyridyl ligand, **L**1. The 4,4′-bis(9,9-dibutyl-7-(3,6-di-*tert*-butyl-9H-carbazol-9-yl)-9H-fluoren-2-yl)-2,2′-bipyridine (**L**1) exhibits two absorption bands, one at around 303 nm and the other one at 322 nm and these characteristic absorption bands exists even in **BPFC** complex but slightly at higher wavelengths. This indicates that the π-π^* transitions in the ancillary bipyridyl ligand, **L**1 are strong and significantly contributing to the high-energy absorption band of **BPFC** complex. The emission spectra of **BPFC** sensitizer was recorded in ethanol by exciting the complex with its absorption maxima of low-energy absorption band. The emission spectrum was analyzed by Gaussian reconvolution method to integrate emission peak to estimate the emission maxima.

Besides the molar extinction coefficient, the other important property, that is, quantity of dye absorped on TiO_2 films and the pattern of dye absorpsion, also influences the light-harvesting capability and the photovoltaic performance of DSSC devices. The molecular diagonal diameter and geometrical structure of any dye vary with respect to π-system substituted on one of the bipyridine moieties of **N**719. As compared to simple 2,2′-bipyridine-4,4′-dicarboxylic acid in **N**3, the 4,4′-bis(9,9-dibutyl-7-(3,6-di-*tert*-butyl-9H-carbazol-9-yl)-9H-fluoren-2-yl)-2,2′-bipyridine in **BPFC** complex largely increases the diagonal molecular size, and hence, it is expected to show significant effect on film absorptions of **BPFC**. Therefore, the film absorption measurements over TiO_2 surface were carried out by staining 7.0 μm thick TiO_2 (18 NRT layered) films

in 0.3 mM dye solutions prepared in ethanol for a period of 16 hours under dark. The absorption spectrum of **BPFC**-sensitized TiO_2 film was recorded and was compared with that of **N**719 sensitized TiO_2 film (Figure 2(b)). The measurements indicate that the dye molecules are anchored on TiO_2 surface, and the film absorbencies for both the dyes are similar. To compare the anchoring pattern and surface morphology of the new sensitizer, the absorbance maxima of low energy absorption band of **BPFC** sensitizer is normalized by the corresponding absorbance maxima of **N**719, while their molar extinction coefficients are normalized by the molar extinction coefficient of **N**719. The film absorbance ratio of **BPFC** calculated is lower than that of **N**719 indicating its lower packing density of the dye molecules on TiO_2 surface. Staining TiO_2 electrodes immediately after sonication of **BPFC** dye solution showed much higher film absorption ratios as compared to those TiO_2 films stained for prolonged soaking times in the **BPFC** dye solutions, and this indicates the necessity of sonication before staining the TiO_2 electrodes, particularly when sensitizers with larger diagonal diameter are employed.

2.4. Electrochemical Properties. In dye-sensitized solar cells, favorite energy offset between dye and titania is a basic requirement for any high-efficiency solar cell, in which the sensitizer's immediate charge generation yield from the excited state has a direct influence on the performance of DSSC device. To measure the electrochemical properties of **BPFC** dye, cyclic voltammetry was employed using tetrabutyl ammonium perchlorate (0.1 M in acetonitrile) as an electrolyte and ferrocene as an internal standard at 0.42 V versus SCE (Figure 3). The oxidation and reduction potentials of **BPFC** are 0.79 V and −0.80 V, respectively. The more positive potential of the sensitizer, relative to I^-/I_3^- redox couple in the electrolyte provide a large thermodynamic driving force for the regeneration of the dye by iodide. Based on absorption and emission spectra, the excitation transition energy (E_{0-0}) of **BPFC** was estimated to be 1.87 eV and the standard potential ($\varphi^0(S+/S^*)$) calculated from the relation of $[\varphi^0(S+/S) = \varphi^0(S+/S^*) - E_{0-0}]$ for the sensitizer was −1.08 V versus SCE. So, $\varphi^0(S+/S^*)$ value is more negative (or higher in energy) than the conduction band edge of TiO_2 providing a thermodynamic driving force to inject electron from the dye to TiO_2.

2.5. Computational Studies. In order to augment the molar extinction coefficient with the π-conjugation extension through 4, 4′-bis(9,9-dibutyl-7-(3,6-di-*tert*-butyl-9H-carbazol-9-yl)-9H-fluoren-2-yl)-2,2′-bipyridine (**L**1) in **BPFC** relative to 2,2′-bipyridine -4,4′-dicarboxylic acid in **N**719 complex, the electronic ground state of fully protonated complex is optimized. To see the influence of the ancillary ligand, **L**1 on the corresponding ruthenium(II) complex, the electronic ground state of the ligand was optimized using B3LYP/6-31G(d) method. Based on the optimized structures, TD-DFT calculations were performed to see the optical properties of the ligand and the corresponding ruthenium(II) complex. The unoccupied (LUMO+4 to LUMO) and occupied (HOMO to HOMO+4) orbitals of **L**1 are shown in Figure 4. The HOMO and HOMO−1 orbitals of **L**1 are degenerate and the π-orbitals are almost delocalized among carbazole modified fluorenes on ancillary bipyridine, which lifts their energy levels. In case of HOMO−2 and HOMO−3, the π-orbitals are almost localized on the carbazole chromophore. In case of LUMO to LUMO+2 orbitals of **L**1, the π^*-orbitals are delocalized over π-system with maximum components on the bipyridine, which depresses their energy levels. LUMO+3 and LUMO+4 have π^*-orbitals localized on carbazole chromophore. The TD-DFT excitation calculations performed for the optimized ground state of the ancillary bipyridyl ligand, **L**1 shows basically two π-π^* transitions with significant oscillation strengths at 303 and 322 nm, respectively, as observed in the case of the absorption spectrum of the ancillary ligand, **L**1.

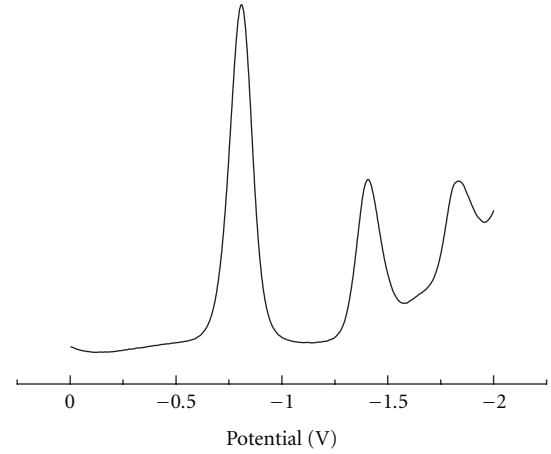

Figure 3: Differential pulse voltammograms of **BPFC**, supporting electrolyte is 0.1 M tetrabutylammonium perchlorate in acetonitrile.

The unoccupied (LUMO to LUMO+4) and occupied (HOMO to HOMO−4) frontier orbitals of **BPFC** are shown in Figure 5. The first three occupied (HOMO to HOMO−2) orbitals of **BPFC** exhibit ruthenium *t*2g character with size mixing from thiocyanate ligand and with π-bonding orbitals of 4,4′-bis(9,9-dibutyl-7-(3,6-di-*tert*-butyl-9H-carbazol-9-yl)-9H-fluoren-2-yl)-2,2′-bipyridine (**L**1). The π-clouds for HOMO−3 orbital for both the dyes are nonbonding combination localized on the NCS ligands. The HOMO−4 and HOMO−5 of **BPFC** are combinations of π-bonding orbitals localized over carbazole moiety of 4,4′-bis(9,9-dibutyl-7-(3,6-di-*tert*-butyl-9H-carbazol-9-yl)-9H-fluoren-2-yl)-2,2′-bipyridine. In HOMO and HOMO−1 orbitals of the new ancillary bipyridine, the π-orbitals are more delocalized over the π-system and bipyridine, and this favors lifting their energy levels. The conjugation length of **BPFC** resulted in increase in the molar extinction coefficient of MLCT absorption bands, which could probably due to lifting their occupied molecular orbitals energy levels as compared to those of **N**719. In case of LUMO, the electron distribution move toward anchoring groups, while assuming similar molecular orbital geometry when adsorbed on TiO_2

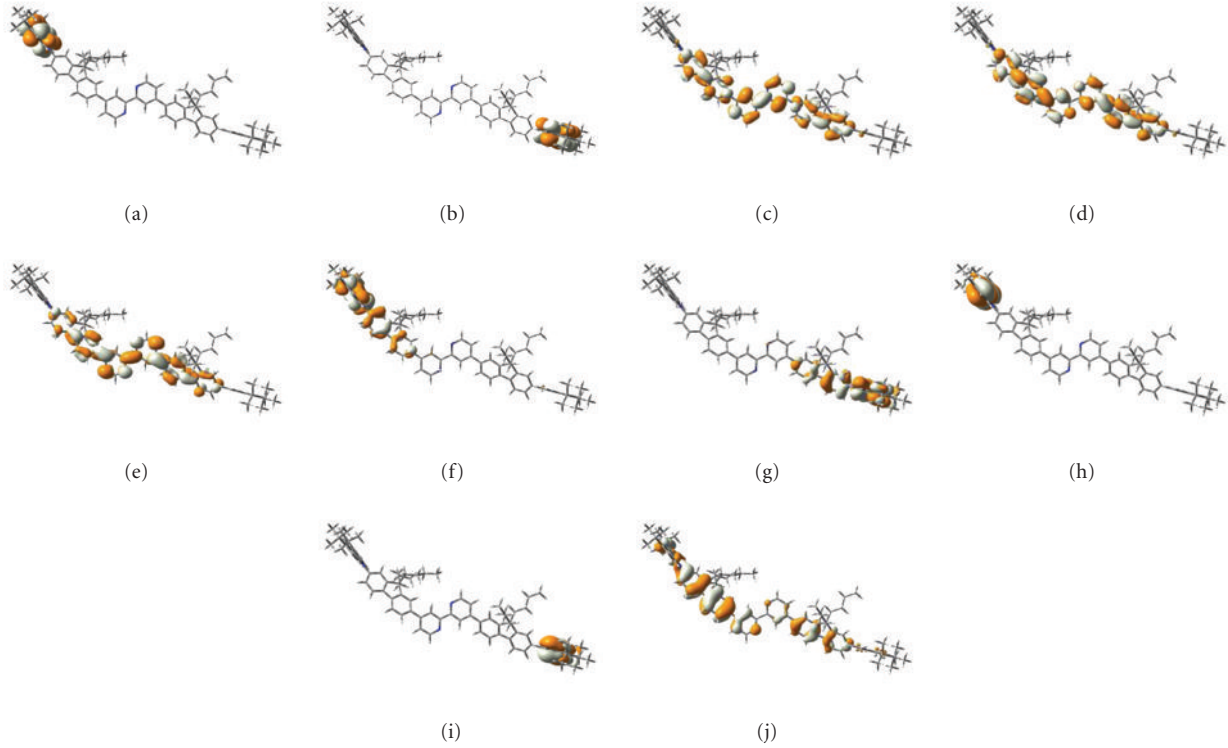

Figure 4: Frontier molecular orbitals of 4,4′-bis(9,9-dibutyl-7-(3,6-di-*tert*-butyl-9H-carbazol-9-yl)-9H-fluoren-2-yl)-2,2′-bipyridine (**L**1); (a) LUMO+4; (b) LUMO+3; (c) LUMO+2; (d) LUMO+1; (e) LUMO; (f) HOMO; (g) HOMO−1; (h) HOMO−2; (i) HOMO−3; (j) HOMO−4.

surface, the close position of the LUMO to the anchoring moieties is expected to enhance the overlap with the 3d orbitals of TiO_2 leading to favored electron injection.

2.6. Thermal Stability. One of the parameters desired to sustain the initial photovoltaic performance of the DSSC over a long period is the high thermal stability of the ruthenium(II) sensitizer. In order to evaluate the thermal stability of the new sensitizer relative to **N**719, TGA analysis were performed using a TGA/SDTA 851^e thermal system (Mettler Toledo, Switzerland) at heating rate of 10°C/min in the temperature range of 50–600°C under N_2 atmosphere (flow rate of 30 mL/min) and the influence of 4,4′-bis(9,9-dibutyl-7-(3,6-di-*tert*-butyl-9H-carbazol-9-yl)-9H-fluoren-2-yl)-2,2′-bipyridine on thermal stability of **BPFC** complex was studied. Film samples ranging from 8 to 10 mg were placed in the sample pan and heated, while weight loss and temperature difference were recorded as a function of temperature. The thermogram of **BPFC** obtained under identical conditions with that of **N**719 was compared. Figure 6 shows the derivative of % conversion with respect to temperature, in which both the thermograms of **BPFC** and **N**719 initially follow similar trend up to around 200°C and after this, **BPFC** loses its mass quickly and hence a decrease in thermal stability by around 50°C was observed as compared to that of **N**719. This indicates that the substitution of 4,4-bis(9,9-dibutyl-9H-fluorene-2-yl)-[2, 2] bipyridine reduces the thermal stability of the ruthenium(II) sensitizer.

2.7. Photovoltaic Properties. To study the influence of 4,4′-bis(9,9-dibutyl-7-(3,6-di-*tert*-butyl-9H-carbazol-9-yl)-9H-fluoren-2-yl)-2,2′-bipyridine as π-conjugation extension on the photovoltaic performance of DSSC relative to 2,2′-bipyridine-4,4′-bicarboxylic acid, double-layer titania film (9.0 + 4.8 μm) 0.16 cm^2 active area TiO_2 electrodes and high-efficiency liquid electrolyte were employed for fabrication of DSSC test cells. The fabrication and evaluation of DSSC test cells were in accordance to the procedures already reported and the volatile electrolyte, (**E**01) containing 0.05 M I_2, 0.1 M LiI, 0.6 M 1,2-dimethyl-3-*n*-propylimidazolium iodide, 0.5 M 4-*tert*-butylpyridine in acetonitrile solvent was employed [31]. The incident photon-to-current conversion efficiency (IPCE) of the sensitizer plotted as a function of excited wavelength was compared with that of **N**719 sensitized solar cell, fabricated and evaluated under identical conditions (Figure 7). The photocurrent action spectrum of **BPFC** showed broad plateau IPCE spectrum with exceeding IPCE of 55%, while that of **N**719 exhibited maximum IPCE reaching 78%. The **BPFC** sensitizer gives short-circuit photocurrent density (J_{SC}), open-circuit voltage (V_{OC}), and fill factor (ff) of 11.52 $mAcm^2$, 566 mV, and 0.72, respectively, yielding an overall energy conversion efficiency (η) of 4.65%, while the test device fabricated under identical conditions with **N**719 dye gave J_{SC} of 14.36 mA/cm^2, V_{OC} of 640 mV, and ff of 0.71 yielding an overall energy conversion efficiency of 6.5%. When compared to **N**719 sensitized solar cell, **BPFC**-sensitized solar cell is expected to show lower power

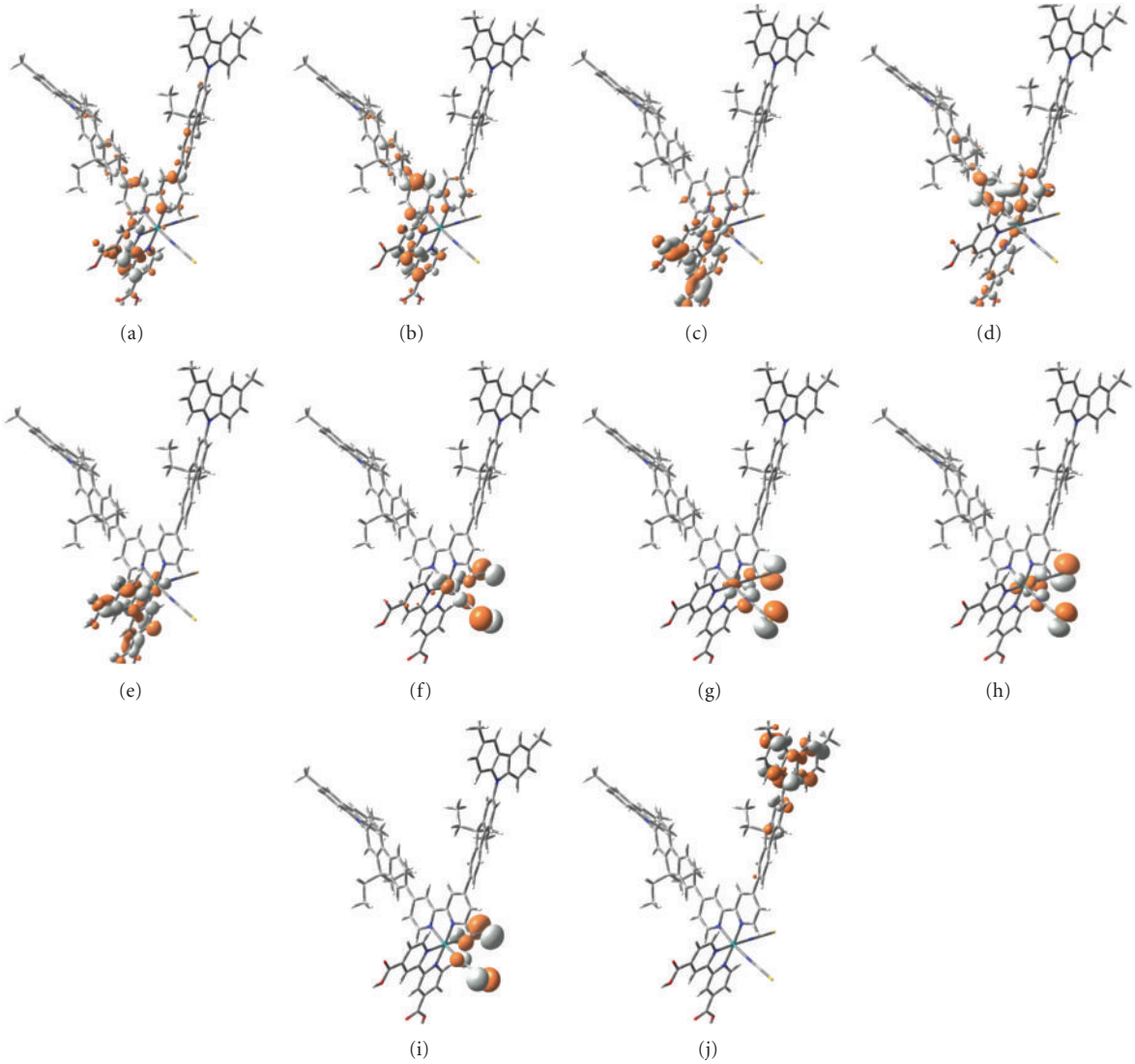

Figure 5: Frontier molecular orbitals of **BPFC**: (a) LUMO+4; (b) LUMO+3; (c) LUMO+2; (d) LUMO+1; (e) LUMO; (f) HOMO; (g) HOMO−1; (h) HOMO−2; (i) HOMO−3; (j) HOMO−4.

Table 1: Detailed photovoltaic parameters of DSSCs.

Sensitizer	J_{SC} (mA/cm^2)	V_{OC} (mV)	ff	Efficiency (%)
BPFC	11.52	566	0.72	4.6
N719	14.36	640	0.71	6.5

Short-circuit photocurrent density (J_{SC}), open-circuit photovoltage (V_{OC}), fill factor (ff).

conversion efficiency due to lower J_{SC} and lower IPCE of **BPFC** relative to that of **N**719 Table 1.

3. Conclusions

The new sensitizer **BPFC** was carefully designed considering the following (1) The alkylgroups (two *n*-butyl and two *t*-butyl on each pyridyl of ancillary ligand) not only increase the solubility of the sensitizer in organic solvents but also serve as electron donating apart from inhibiting water induced desorption of the sensitizer from the TiO_2. (2) Carbazole is a triarylamine equivalent which is known to improve the efficiency of the sensitizer. (3) The biphenyl group in Fluorene moiety serves as extended conjugation for enhancing the molar extinction coefficient and provides aromatic stability to the molecule. (4) The bipyridine dicarboxylic acid provides excellent anchoring of the complex on to the TiO_2 surface facilitating easy electron injection. Thus, the multiple performance increasing features of the **BPFC** sensitizer makes the ruthenium(II) complex unique for DSSC application and showed solar-to-electric energy conversion efficiency (η) 4.6%, while under similar fabrication and measurement conditions, standard **N**719 showed 6.5% efficiency. The new ruthenium(II) bipyridyl sensitizer showed relatively high molar extinction coefficient. Upon

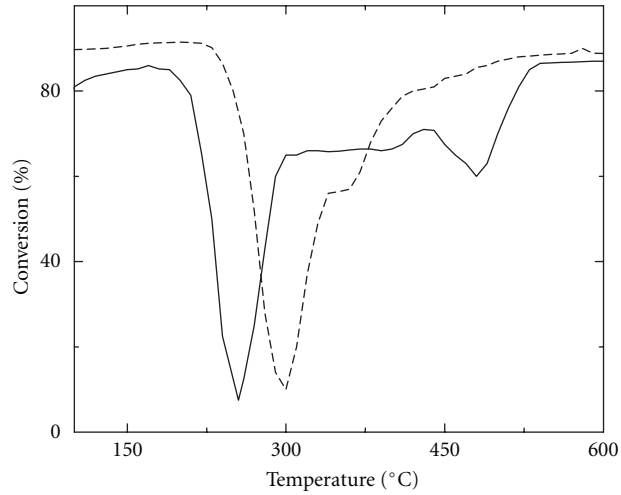

Figure 6: TG-thermograms of **BPFC** (—) relative to **N**719 (----).

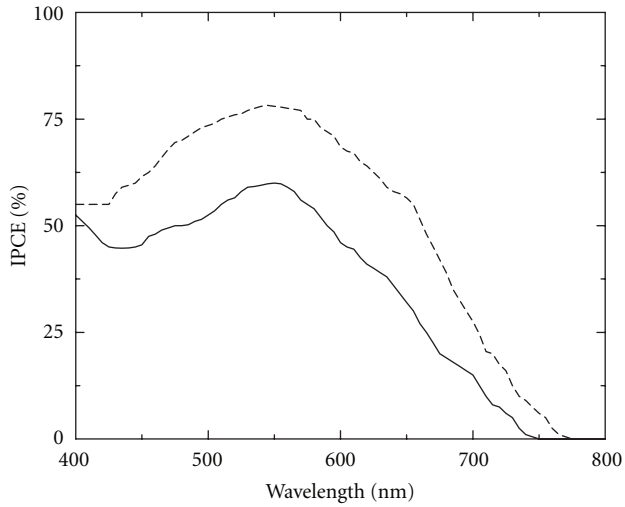

Figure 7: Photocurrent action spectra of DSSC constructed based on **BPFC** (—) and **N**719 (----) sensitizers.

sensitization with nano-crystalline TiO_2, the dye showed decreased film absorption ratios, whereas staining the TiO_2 electrodes with freshly sonicated dye solutions showed relatively increased film absorption ratios on TiO_2 surface. The lower solar-to-electrical energy conversion efficiency could be result of lower IPCE value and lower film absorption ratios. Design and development of super sensitizers with similar high performance features but with less bulky nature are under progress.

Acknowledgments

C. S. Rao thanks IICT-AIC collaborative project for a fellowship. T. Suresh thanks CSIR, New Delhi, for senior research fellowship. M. Chandrasekharam thanks DST, New Delhi for the grant of the project entitled "Advancing the efficiency and production potential of Excitonic Solar Cells (APEX)" under UK-DST consortium.

References

[1] A. Hagfeldt, G. Boschloo, L. Sun, L. Kloo, and H. Pettersson, "Dye-sensitized solar cells," *Chemical Reviews*, vol. 110, no. 11, pp. 6595–6663, 2010.

[2] A. Hagfeld and M. Grätzel, "Light-induced redox reactions in nanocrystalline systems," *Chemical Reviews*, vol. 95, no. 1, pp. 49–68, 1995.

[3] K. Hara, M. Kurashige, S. Ito et al., "Novel polyene dyes for highly efficient dye-sensitized solar cells," *Chemical Communications*, vol. 9, no. 2, pp. 252–253, 2003.

[4] S. Ferrere and B. A. Gregg, "Large increases in photocurrents and solar conversion efficiencies by UV illumination of dye sensitized solar cells," *Journal of Physical Chemistry B*, vol. 105, no. 32, pp. 7602–7605, 2001.

[5] S. G. Chen, S. Chappel, Y. Diamant, and A. Zaban, "Preparation of Nb_2O_5 coated TiO_2 nanoporous electrodes and their application in dye-sensitized solar cells," *Chemistry of Materials*, vol. 13, no. 12, pp. 4629–4634, 2001.

[6] B. O'Regan and M. Grätzel, "A low-cost, high-efficiency solar cell based on dye-sensitized colloidal TiO_2 films," *Nature*, vol. 353, no. 6346, pp. 737–740, 1991.

[7] M. Grätzel, "Photoelectrochemical cells," *Nature*, vol. 414, no. 6861, pp. 338–344, 2001.

[8] M. K. Nazeeruddin, A. Kay, I. Rodicio et al., "Conversion of light to electricity by cis-X2bis(2,2'-bipyridyl-4,4'-dicarboxylate)ruthenium(II) charge-transfer sensitizers (X = Cl-, Br-, I-, CN-, and SCN-) on nanocrystalline titanium dioxide electrodes," *Journal of the American Chemical Society*, vol. 115, no. 14, pp. 6382–6390, 1993.

[9] S. M. Zakeeruddin, M. K. Nazeeruddin, R. Humpry Baker et al., "Design, synthesis, and application of amphiphilic ruthenium polypyridyl photosensitizers in solar cells based on nanocrystalline TiO_2 films," *Langmuir*, vol. 18, no. 3, pp. 952–954, 2002.

[10] P. Wang, S. M. Zakeeruddin, J. E. Moser, M. K. Nazeeruddin, T. Sekiguchi, and M. Grätzel, "A stable quasi-solid-state dye-sensitized solar cell with an amphiphilic ruthenium sensitizer and polymer gel electrolyte," *Nature Materials*, vol. 2, no. 6, pp. 402–407, 2003.

[11] P. Wang, S. M. Zakeeruddin, J. E. Moser et al., "Stable new sensitizer with improved light harvesting for nanocrystalline dye-sensitized solar cells," *Advanced Materials*, vol. 16, no. 20, pp. 1806–1811, 2004.

[12] P. Wang, C. Klein, R. Humphry-Baker, S. M. Zakeeruddin, and M. Grätzel, "A high molar extinction coefficient sensitizer for stable dye-sensitized solar cells," *Journal of the American Chemical Society*, vol. 127, no. 3, pp. 808–809, 2005.

[13] D. Kuang, C. Klein, S. Ito et al., "High molar extinction coefficient ion-coordinating ruthenium sensitizer for efficient and stable mesoscopic Dye-sensitized solarCells," *Advanced Functional Materials*, vol. 17, pp. 154–160, 2007.

[14] K. J. Jiang, N. Masaki, J. B. Xia, S. Noda, and S. Yanagida, "A novel ruthenium sensitizer with a hydrophobic 2-thiophen-2-yl-vinyl- conjugated bipyridyl ligand for effective dye sensitized TiO_2 solar cells," *Chemical Communications*, no. 23, pp. 2460–2462, 2006.

[15] C.-Y. Chen, S.-J. Wu, C.-G. Wu, J.-G. Chen, and K.-C. Ho, "A ruthenium complex with superhigh light-harvesting capacity for dye-sensitized solar cells," *Angewandte Chemie—International Edition*, vol. 118, pp. 5954–5957, 2006.

[16] D. Kuang, C. Klein, S. Ito et al., "High effiiciency and stable mesoscopic Dye-sensitized solar cells based on a high

molar extinction cofficient Ru-sensitizer and non-volatile electrolyte," *Advanced Materials*, vol. 19, pp. 1133–1137, 2007.

[17] D. Kuang, C. Klein, Z. Zhang et al., "Stable, high-efficiency ionic-liquid-based mesoscopic dye-sensitized solar cells," *Small*, vol. 3, no. 12, pp. 2094–2102, 2007.

[18] F. Matar, T. H. Ghaddar, K. Walley, T. DosSantos, J. R. Durrant, and B. O'Regan, "A new ruthenium polypyridyl dye, TG6, whose performance in dye-sensitized solar cells is surprisingly close to that of N719, the 'dye to beat' for 17 years," *Journal of Materials Chemistry*, vol. 18, no. 36, pp. 4246–4253, 2008.

[19] Y. Cao, Y. Bai, Q. Yu et al., "Dye-sensitized solar cells with a high absorptivity ruthenium sensitizer featuring a 2-(hexylthio)thiophene conjugated bipyridine," *Journal of Physical Chemistry C*, vol. 113, no. 15, pp. 6290–6297, 2009.

[20] F. Gao, Y. Cheng, Q. Yu et al., "Conjugation of selenophene with bipyridine for a high molar extinction coefficient sensitizer in dye-sensitized solar cells," *Inorganic Chemistry*, vol. 48, no. 6, pp. 2664–2669, 2009.

[21] F. Gao, Y. Wang, D. Shi et al., "Enhance the optical absorptivity of nanocrystalline TiO_2 film with high molar extinction coefficient ruthenium sensitizers for high performance dye-sensitized solar cells," *Journal of the American Chemical Society*, vol. 130, no. 32, pp. 10720–10728, 2008.

[22] M. Chandrasekharam, C. Srinivasarao, T. Suresh et al., "High spectral response heteroleptic ruthenium (II) complexes as sensitizers for dye sensitized solar cells," *Journal of Chemical Sciences*, vol. 123, pp. 37–46, 2011.

[23] P. Y. Reddy, L. Giribabu, C. Lyness et al., "Efficient sensitization of nanocrystalline TiO_2 films by a near-IR-absorbing unsymmetrical zinc phthalocyanine," *Angewandte Chemie—International Edition*, vol. 46, no. 3, pp. 373–376, 2007.

[24] L. Giribabu, M. Chandrasekheram, M. L. Kantham et al., "Conjugated organic dyes for dye-sensitized solar cells," *Indian Journal of Chemistry—Section A*, vol. 45, no. 3, pp. 629–634, 2006.

[25] M. D. Iosip, S. Destri, M. Pasini, W. Porzio, K. P. Pernstich, and B. Batlogg, "New dithieno[3,2-b:2',3'-d]thiophene oligomers as promising materials for organic field-effect transistor applications," *Synthetic Metals*, vol. 146, no. 3, pp. 251–257, 2004.

[26] E. J. Meijer, A. V. G. Mangnus, B. H. Huisman, G. W. 'T Hooft, D. M. de Leeuw, and T. M. Klapwijk, "Photoimpedance spectroscopy of poly(3-hexyl thiophene) metal-insulator-semiconductor diodes," *Synthetic Metals*, vol. 142, no. 1–3, pp. 53–56, 2004.

[27] Z. H. Li, M. S. Wong, Y. Tao, and J. Lu, "Diphenylamino end-capped oligofluorenes with enhanced functional properties for blue light emission: synthesis and structure-property relationships," *Chemistry—A European Journal*, vol. 11, no. 11, pp. 3285–3293, 2005.

[28] L. Giribabu, C. Vijay Kumar, C. S. Rao et al., "High molar extinction coefficient amphiphilic ruthenium sensitizers for efficient and stable mesoscopic Dye-sensitized solar cells," *Energy and Environmental Science*, vol. 2, no. 7, pp. 770–773, 2009.

[29] M. Chandrasekharam, G. Rajkumar, C. Srinivasa Rao, T. Suresh, and P. Yella Reddy, "Phenothiazine conjugated bipyridine—a new class of ancillary ligand for Ru-sensitizer in Dye sensitized solar cell application," *Synthetic Metals*. In press.

[30] M. Chandrasekharam, G. Rajkumar, C. Srinivasa Rao et al., "Molecular engineered fluorene substituted Ru-complex for efficient mesoscopic dye sensitized solar cells," vol. 2, 2011, *Advances in Natural Sciences: Nanoscience and Nanotechnology*. Accepted.

[31] M. Chandrasekharam, G. Rajkumar, C. Srinivasa Rao et al., "Polypyridyl Ru(II)-sensitizers with extended π-system enhances the performance of Dye sensitized solar cells," *Synthetic Metals*, vol. 161, pp. 1098–1104, 2011.

[32] M. Chandrasekharam, G. Rajkumar, C. Srinivasa Rao, P. Yella Reddy, and M. Lakshmi Kantam, "Change of Dye bath for sensitisation of nanocrystalline TiO_2 films: enhances performance of Dye-sensitized solar cells," *Advances in OptoElectronics*, vol. 2011, Article ID 376369, 9 pages.

[33] C.-Y. Chen, J.-G. Chen, S.-J. Wu, J.-Y. Li, C.-G. Wu, and K.-C. Ho, "Multifunctionalized ruthenium-based supersensitizers for highly efficient dye-sensitized solar cells," *Angewandte Chemie—International Edition*, vol. 47, no. 38, pp. 7342–7345, 2008.